Global robust attitude tracking with torque disturbance rejection via dynamic hybrid feedback ⋆

Davide Invernizzi [a], Marco Lovera [a], Luca Zaccarian [b,c]

[a] *Politecnico di Milano, Department of Aerospace Science and Technology, Via La Masa 34, 20156, Milano*

[b] *CNRS, LAAS, 7 avenue du colonel Roche, F-31400 Toulouse, France*

[c] *University of Trento, Dipartimento di Ingegneria Industriale, Via Sommarive 9, 38123 Povo, Italy*

Abstract

In this paper an approach to the design of robust global attitude tracking controllers for fully actuated rigid bodies is proposed. The challenge of simultaneously dealing with topological obstructions to global attitude tracking and with disturbances affecting the attitude dynamics is tackled by means of a hybrid hierarchical design that exploits the cascade structure of the underlying mathematical model. The proposed hierarchical strategy is based on an inner-outer loop paradigm comprising a dynamic control law for angular velocity tracking (inner loop) and a hybrid control law for attitude tracking (outer loop). By leveraging recent tools for the stability analysis of hybrid systems, we prove a robust global tracking property by assuming mild properties on the dynamics of the velocity feedback. We also discuss a few relevant examples satisfying these properties, encompassing harmonic disturbance compensators and conditional integrators, capable of rejecting unknown constant disturbances with an intrinsic anti-windup action.

1 Introduction

Attitude tracking is a well-known problem yet it is still an active topic of research, with applications in aerospace, robotics and underwater vehicles, to name a few. Robust control designs based on continuous time-invariant control laws guarantee at best an almost global stability result due to topological obstructions of the three-dimensional special orthogonal group (SO(3)) [10,12,11,8]. When looking for a global solution to the problem, discontinuous or hybrid control designs are needed [13]. While controllers with global guarantees have been developed in the last decade by leveraging recent tools of hybrid control theory [7], most of the designs neglect disturbance torques [13,2,6] or they only consider constant disturbances [19,11].

In this work we extend the smooth hierarchical control design of our preliminary work [8] to achieve global tracking in the presence of disturbances through dynamic hybrid feedback. The hierarchical architecture is built upon the cascade structure of the model for rigid-body attitude control to split the problem of designing a robust and global controller in two simpler subproblems: A) stabilization of the attitude kinematics, whose model is exact but evolves on a nonlinear manifold and B) stabilization of the angular velocity dynamics, which evolves in a Euclidean space but is affected by unknown disturbances and model uncertainties. To implement such ideas, the control law that we develop relies on an inner-outer loop paradigm where: a quaternion-based proportional control law is employed for kinematic tracking (inner loop); a dynamic control law based on the internal model principle is employed to reject exogenous disturbances while ensuring angular velocity tracking (outer loop); a hybrid logic is implemented to ensure global tracking results while avoiding the unwinding phenomenon [13]. The main advantage of the proposed control law over existing formulations is that one can deal with the design of the inner loop controller by referring to the angular velocity dynamics alone: the challenging part of attitude control (related to topological obstructions) is handled by the outer loop controller. Indeed, most designs exploiting a dynamic control law for disturbance rejection deal with the case of constant disturbances [19,11,12] and rely on the development of sophisticated Lyapunov functions [19,11,12] which in-

⋆ This work was partially supported: by the Italian Ministry for Research in the framework of the 2020 Program for Research Projects of National Interest (PRIN), under Grant 2020RTWES4; by ANR via grant HANDY, number ANR-18-CE40-0010.

Email addresses: davide.invernizzi@polimi.it (Davide Invernizzi), marco.lovera@polimi.it (Marco Lovera), zaccarian@laas.fr (Luca Zaccarian).

volve mixed terms among the kinematic and dynamic states, sometimes leading to important constraints on the gains [11,12], and thereby affecting the achievable performance. The increased architectural complexity of our solution is balanced by the possibility of focusing on the development of individual Lyapunov functions for the inner and outer loop dynamics. This simplifies the use of non-trivial dynamic controllers in the inner loop, capable of compensating for the effect of classes of exogenous disturbances of interest.

Exploiting an internal model approach to obtain an autonomous characterization of the perturbed angular velocity error dynamics (inner loop), which takes the form of a differential inclusion, and then relying on invariance principles for hybrid inclusions [18], our control design allows proving global tracking, *e.g.*, when using a harmonic compensator or when using conditional integrators [4], which are nonlinear integral controllers embedding an anti-windup action. The outer loop controller that we adopt here is based on the stabilizer proposed in [15] exploiting the quaternions parametrization, the use of which is widespread in aerospace applications. While quaternion-based controllers require a consistent path-lifting extraction algorithm to avoid undesired phenomena as shown in [14], they provide simplified expressions of the control logic over synergistic rotation matrix-based stabilizers [15,3] and allow us to focus on the development of the inner loop controllers, which is the main objective of this work. Nonetheless, we underline that recently developed hybrid stabilizers exploiting alternative parametrizations ([1,3,5]) could be used within our hierarchical construction with minor adjustments.

Notation. We report below some essential notation.
1) Vectors. $\mathbb{R}\,(\mathbb{R}_{>0}, \mathbb{R}_{\geq 0})$ denotes the set of (positive, nonnegative) real numbers, $\mathbb{R}^n$ denotes the n-dimensional Euclidean space and $\mathbb{R}^{m\times n}$ the set of $m\times n$ real matrices. The i-th vector of the canonical basis in $\mathbb{R}^n$, *i.e.*, the vector with a 1 in the i-th coordinate and 0's elsewhere, is denoted as e_i and the identity matrix in $\mathbb{R}^{n\times n}$ is $I_n := [e_1 \cdots e_i \cdots e_n]$. Given a bound $M \in \mathbb{R}_{>0}$, the symmetric saturation function is defined as $\mathrm{sat}_M(x) := \min(\max(-M, x), M)$ for $x \in \mathbb{R}$ while its unit version ($M = -m = 1$) is simply denoted with $\mathrm{sat}(x) := \mathrm{sat}_1(x)$. The decentralized vector saturation function is also denoted $\mathrm{sat}(\cdot)$ and $\mathrm{sat}_M(\cdot)$ with a slight abuse of notation.
2) Rotation matrices and quaternions. The set $\mathrm{SO}(3) := \{R \in \mathbb{R}^{3\times 3} : R^\top R = I_3, \det(R) = 1\}$ denotes the three-dimensional Special Orthogonal group. Given $\omega \in \mathbb{R}^3$, the map $S\cdot : \mathbb{R}^3 \to \mathbb{R}^3 := \{\Omega \in \mathbb{R}^{3\times 3} : \Omega = -\Omega^\top\}$ is such that $S(\omega)y = \omega \times y$, $\forall y \in \mathbb{R}^3$ where $\times$ represents the cross product in $\mathbb{R}^3$. The attitude kinematics can be lifted by parametrizing SO(3) with unit quaternions, which live in $\mathbb{S}^3 := \{q \in \mathbb{R}^4 : q^\top q = 1\}$, through the formula $\mathcal{R} : \mathbb{S}^3 \mapsto \mathrm{SO}(3)$ defined as $\mathcal{R}(q) := I_3 + 2\eta S(\epsilon) + 2S(\epsilon)^2$ where $\eta \in \mathbb{R}$, $\epsilon \in \mathbb{R}^3$ are the scalar and vector components of the quaternion $q = \left[\begin{smallmatrix}\eta & \epsilon^\top\end{smallmatrix}\right]^\top$, respectively. We recall that for every $R \in \mathrm{SO}(3)$ there exist two antipodal unit quaternions $\pm q$, namely, $\mathcal{R}(q) = \mathcal{R}(-q)$: the mapping $\mathcal{R}(\cdot)$ is everywhere a local diffeomorphism but globally a two-to-one mapping. Multiplication between two quaternions is given by the quaternion product $\circ : \mathbb{S}^3 \times \mathbb{S}^3 \mapsto \mathbb{S}^3$ such that: $q_1 \circ q_2 := \left[\begin{smallmatrix}\eta_1 & -\epsilon_1^\top \\ \epsilon_1 & \eta_1 I_3 + S(\epsilon_1)\end{smallmatrix}\right]\left[\begin{smallmatrix}\eta_2 \\ \epsilon_2\end{smallmatrix}\right]$. The quaternion $q_I := \left[\begin{smallmatrix}1 & 0 & 0 & 0\end{smallmatrix}\right]^\top$ satisfies $q \circ q_I = q_I \circ q$ for any $q \in \mathbb{S}^3$ and is called the identity element. It can be verified that for each $q = \left[\begin{smallmatrix}\eta & \epsilon^\top\end{smallmatrix}\right]^\top$, the inverse quaternion $q^{-1} = \left[\begin{smallmatrix}\eta & -\epsilon^\top\end{smallmatrix}\right]^\top$ satisfies and $q \circ q^{-1} = q^{-1} \circ q = q_I$. Finally, given any two quaternions q_1, q_2, $\mathcal{R}(q_1)\mathcal{R}(q_2) = \mathcal{R}(q_1 \circ q_2)$, and given any vector $v \in \mathbb{R}^3$ and any quaternion $q \in \mathbb{S}^3$, $q^{-1} \circ \left[\begin{smallmatrix}0 \\ v\end{smallmatrix}\right] \circ q = \left[\begin{smallmatrix}0 \\ \mathcal{R}(q)v\end{smallmatrix}\right]$.
3) Hybrid dynamical systems. According to [7], a hybrid dynamical system comprises a *flow map* $F : \mathbb{R}^n \rightrightarrows \mathbb{R}^n$ that can be evaluated in a *flow set* $C \subset \mathbb{R}^n$ and similarly a *jump map* $G : \mathbb{R}^n \rightrightarrows \mathbb{R}^n$ and a *jump set* $D \subset \mathbb{R}^n$. Solutions to hybrid dynamical systems take values on *hybrid time domains* $E \subset \mathbb{R}_{\geq 0} \times \mathbb{N}$ corresponding to the union of infinitely many sets $[t_j, t_{j+1}] \times j$, $j \in \mathbb{N}$ where $0 = t_0 \leq t_1 \leq t_2 \leq \ldots$, or of finitely many of such sets, with $[t_j, t_{j+1}] \times j$, $[t_j, t_{j+1}) \times j$ or $[t_j, \infty) \times j$.

2 Rigid body attitude control problem

Consider an inertial reference frame and a body-fixed frame whose origin is located at the center of mass of a rigid body. The attitude dynamics of the rigid body is described by the equations:

$$\dot{R} = RS(\omega) \tag{1}$$
$$J\dot{\omega} = -S(\omega)J\omega + \tau_c + \tau_e \tag{2}$$

where $R \in \mathrm{SO}(3)$ is the rotation matrix describing the attitude of the body-fixed frame, $\omega \in \mathbb{R}^3$ is the angular velocity, $J = J^\top \in \mathbb{R}^{3\times 3}_{>0}$ is the inertia matrix with respect to the center of mass, $\tau_c \in \mathbb{R}^3$ is the control torque exerted by the actuators and $\tau_e \in \mathbb{R}^3$ is the disturbance torque accounting for unknown exogenous effects, all expressed in the body frame. The objective of this work is to introduce dynamic controllers to globally solve the attitude tracking problem for a fully actuated rigid body in the presence of disturbances τ_e. Before proceeding, let us consider the following standard assumption.

Assumption 1 *The desired trajectory $t \mapsto (R_d(t), \omega_d(t)) \in \mathrm{SO}(3) \times \mathbb{R}^3$ satisfies $\dot{R}_d(t) = R_d(t)S(\omega_d(t))$ $\forall t \geq 0$ and $t \mapsto \omega_d(t)$ is continuously differentiable and uniformly bounded.*

The state feedback dynamic attitude tracking problem can then be formalized as follows.

Problem 1 *Consider the attitude dynamics in equations* (1)-(2). *Given a desired trajectory* $t \mapsto (R_d(t), \omega_d(t)) \in \mathrm{SO}(3) \times \mathbb{R}^3$ *satisfying Assumption 1, design a state-feedback dynamic controller delivering a control torque* $\tau_c \in \mathbb{R}^3$ *such that the trajectory* $t \mapsto (R_d(t), \omega_d(t))$ *is globally asymptotically tracked, robustly with respect to the disturbance torque generated by the exosystem*

$$\dot{w} = s(w), \quad \tau_e = \tau(w), \quad w \in \mathcal{W} \tag{3}$$

where $\mathcal{W}$ *is a nonempty compact set and where* τ_e *is not available for measurement.*

The class of torques described through the exosystem (3) includes several kinds of disturbances of engineering interest (*e.g.*, constant, ramp-like, harmonic). The solution to Problem 1 proposed in this work relies on an internal model principle, requires the knowledge of the exosystem in (3) and of the velocity ω_d and acceleration $\dot{\omega}_d$ of the reference trajectory.

3 Control law design and stability analysis

In this section a hierarchical control architecture solving Problem 1 is presented. The proposed solution is based on an inner-outer loop paradigm and gives freedom in selecting different stabilizers of the inner and outer loops.

3.1 Control architecture, closed-loop error dynamics

As motivated in the introduction, we use unit quaternions to parametrize the attitude of the rigid body. Accordingly, the kinematics (1) is "lifted" onto $\mathbb{S}^3$ as

$$\dot{q} = \frac{1}{2} q \circ \left[\begin{smallmatrix} 0 \\ \omega \end{smallmatrix} \right] = W(q)\omega, \tag{4}$$

where $q = \left[\begin{smallmatrix} \eta & \epsilon^\top \end{smallmatrix} \right]^\top \in \mathbb{S}^3$, $W(q) := \frac{1}{2} \left[\begin{smallmatrix} -\epsilon^\top \\ \eta I_3 + S(\epsilon) \end{smallmatrix} \right]$ and $t \mapsto q(t)$ satisfies $\mathcal{R}(q(t)) = R(t)\ \forall t \geq t_0$. Equation (4) can be split in the scalar part $\eta \in \mathbb{R}$ and the vector part $\varepsilon \in \mathbb{R}^3$ of the quaternion as $\dot{\eta} = -\frac{1}{2}\epsilon^\top \omega$, $\dot{\varepsilon} = \frac{1}{2}\left(\eta I_3 + S(\epsilon)\right)\omega$. The tracking Problem 1 can be cast as a stabilization problem by introducing suitable error coordinates. To this aim, let the quaternion error be defined as

$$q_e := q_d^{-1} \circ q = \left[\begin{smallmatrix} \eta_e \\ \varepsilon_e \end{smallmatrix} \right] \in \mathbb{S}^3, \tag{5}$$

where $t \mapsto q_d(t)$ is a continuously differentiable function satisfying $\dot{q}_d = W(q_d)\omega_d$ and $\mathcal{R}(q_d(t)) = R_d(t)$ for all $t \geq t_0$. As for the the angular velocity error, consider

$$\omega_e := \omega_v - \omega \in \mathbb{R}^3, \tag{6}$$

where ω_v is a virtual angular velocity to be assigned by the outer loop of the controller. The velocity error (6) that we consider is different from existing approaches where $\omega_e = \omega - R_e^\top \omega_d$ is usually employed [13]. The selection (6) is motivated by our hierarchical construction, as clarified in the following.

To solve Problem 1, we design the control torque τ_c as the output of the following hybrid dynamic controller having a continuous state x_c and a logical state $h \in \{-1, 1\}$:

$$\left.\begin{aligned} \dot{x}_c &= \gamma_c(x_c, \omega_e, \omega_v) \\ \dot{h} &= 0 \end{aligned}\right\} \qquad (h, q_e, \omega_e) \in C \tag{7a}$$

$$\left.\begin{aligned} x_c^+ &= x_c \\ h^+ &= -h \end{aligned}\right\} \qquad (h, q_e, \omega_e) \in D \tag{7b}$$

$$\tau_c = S(\omega)J\omega + J\omega_{vd} + \gamma_\omega(x_c, \omega_e, \omega_v) \tag{7c}$$

where

$$\omega_v := \gamma_q(h, q_e) + R_e^\top \omega_d \tag{8}$$

$$\begin{aligned} \omega_{vd} = {} & \tfrac{1}{2} h K_R \left(\eta_e I_3 + S(\varepsilon_e)\right)\left(\omega_e - \gamma_q(h, q_e) + \right. \\ & \left. + S(\omega_e - \gamma_q(h, q_e)) R_e^\top \omega_d + R_e^\top \dot{\omega}_d. \right. \end{aligned} \tag{9}$$

In (8)-(9), $R_e := \mathcal{R}(q_e) = \mathcal{R}(q_d^{-1} \circ q) = \mathcal{R}(q_d^{-1})\mathcal{R}(q) = R_d^\top R$ is the rotation matrix describing the relative error between the frames associated with R_d and R, $\gamma_q(\cdot, \cdot) : \{-1, 1\} \times \mathbb{S}^3 \to \mathbb{R}^3$, $\gamma_\omega(\cdot, \cdot, \cdot) : \mathbb{R}^{n_c} \times \mathbb{R}^3 \times \mathbb{R}^3 \to \mathbb{R}^3$, $\gamma_c(\cdot, \cdot, \cdot) : \mathbb{R}^{n_c} \times \mathbb{R}^3 \times \mathbb{R}^3 \to \mathbb{R}^3$ are stabilizers to be designed. The overall state $x_a := (h, q_e, \omega_e, x_c)$ of the error dynamics belongs to the manifold $\chi := \{-1, 1\} \times \mathbb{S}^3 \times \mathbb{R}^3 \times \mathbb{R}^{n_c}$. The flow and jump sets C and D will be specified in Section 3.3: here we emphasize that these sets do not depend on x_c. The hierarchical structure of controller (7a)–(7c) is clearly visible in Figure 1: the control torque τ_c (inner loop) is in charge of tracking the virtual angular velocity input ω_v (equation (8)) provided by the outer loop. The outer loop controller comprises a feedforward term related to the desired angular velocity reference $t \mapsto \omega_d(t)$ and a kinematic stabilizer

$$\gamma_q(h, q_e) := -hK_R \varepsilon_e. \tag{10}$$

Using the angle-axis representation $(\phi, n) \in (-\pi, \pi] \times \mathbb{S}^2$, since $q_e = \left[\begin{smallmatrix} \cos(\frac{\phi}{2}) & n \sin(\frac{\phi}{2}) \end{smallmatrix} \right]^\top$, stabilizer (10) acts as a proportional-like controller $\tilde{\gamma}_q(n, \phi) = -h \sin(\frac{\phi}{2}) K_R n$.

Remark 1 *The additional state* x_c *is included in our architecture to allow for the use of dynamic controllers, such as PIDs, often necessary in practical applications, where the disturbance* τ_e *may comprise an unknown bias to be compensated. Two relevant cases will be presented in Section 4, a different one can be found in [8].*

The closed-loop error dynamics obtained by using (5), (7), (10) and (2)-(4) is characterized by the following proposition, stated without proof for space limitations.

Proposition 1 *Consider the plant dynamics* (2)-(4) *and the dynamic controller* (7). *Using the tracking errors*

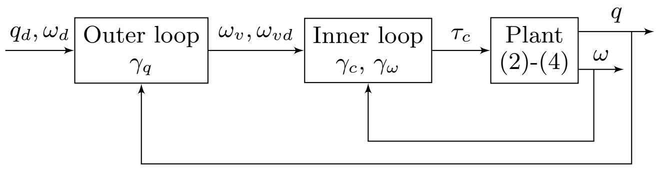

Fig. 1. Proposed inner-outer loop control architecture.

in (5)-(6)*, we have* $\dot{\omega}_v \equiv \omega_{vd}$ *along all flowing solutions. Moreover, the closed-loop dynamics reads*

$$\left.\begin{aligned} \dot{q}_e &= -W(q_e)(hK_R\varepsilon_e + \omega_e) \\ J\dot{\omega}_e &= -\gamma_\omega(x_c, \omega_e, \omega_v) - \tau_e \\ \dot{x}_c &= \gamma_c(x_c, \omega_e, \omega_v) \\ \dot{h} &= 0 \end{aligned}\right\} \quad (h, q_e, \omega_e) \in C \tag{11a}$$

$$\left.\begin{aligned} q_e^+ &= q_e \\ \omega_e^+ &= \omega_e + 2hK_R\varepsilon_e \\ x_c^+ &= x_c \\ h^+ &= -h \end{aligned}\right\} \quad (h, q_e, \omega_e) \in D. \tag{11b}$$

3.2 Exosystem and error dynamics

For a suitable rejection of the disturbance τ_e in (2) our control law is designed by following the regulation theory approach where τ_e originates from an exosystem as defined in (3). Then, τ_e can be regarded as an internal signal of an autonomous description of the error dynamics. To illustrate the regulation approach, consider the elementary case of a scalar system $\dot{x} = u + d$, where the disturbance is generated by the exosystem $\dot{w} = 0$, $d = w$. Using the control law $\dot{x}_c = x$, $u = -k_p x - k_i x_c$, the change of coordinates $\tilde{x}_c = x_c - w/k_i$ results in the autonomous closed-loop system $\dot{x} = -k_p x - k_i(\tilde{x}_c + w/k_i) + w = -k_p x - k_i \tilde{x}_c$, $\dot{\tilde{x}}_c = x - \dot{w}/k_i = x$. Generalizing this idea, one can typically define a shifted set of coordinates $\tilde{x}_c = x_c - \psi(w)$ for some function $\psi(\cdot)$ such that the following set-valued nonlinear regulator equations are satisfied for all $(\tilde{x}_c, \omega_e, \omega_v, w) \in \mathbb{R}^{n_c} \times \mathbb{R}^3 \times \mathbb{R}^3 \times \mathcal{W}$,

$$\gamma_c(\tilde{x}_c + \psi(w), \omega_e, \omega_v) - \mathrm{D}\psi s(w) \in \Gamma_c(\tilde{x}_c, \omega_e, \omega_v) \tag{12}$$
$$\gamma_\omega(\tilde{x}_c + \psi(w), \omega_e, \omega_v) + \tau(w) \in \Gamma_\omega(\tilde{x}_c, \omega_e, \omega_v) \tag{13}$$

for some suitable set-valued maps $\Gamma_c(\cdot,\cdot,\cdot) : \mathbb{R}^{n_c} \times \mathbb{R}^3 \times \mathbb{R}^3 \rightrightarrows \mathbb{R}^3$, $\Gamma_\omega(\cdot,\cdot,\cdot) : \mathbb{R}^{n_c} \times \mathbb{R}^3 \times \mathbb{R}^3 \rightrightarrows \mathbb{R}^3$. In some simpler scenarios, one may have $\Gamma_c(\tilde{x}_c, \omega_e, \omega_v) = \{\gamma_c(\tilde{x}_c, \omega_e, \omega_v)\}$ and $\Gamma_\omega(\tilde{x}_c, \omega_e, \omega_v) = \{\gamma_\omega(\tilde{x}_c, \omega_e, \omega_v)\}$ (this is the case discussed in Section 4.1). However, more sophisticated solutions, such as that of Section 4.2, require the nontrivial set-valued inclusion in (12)–(13). Moreover, we only require (mild) regularity properties of maps Γ_c and Γ_ω, so that even discontinuous selections of γ_c and γ_ω (suitably embedded in Γ_c and Γ_ω, possibly through a Filippov regularization) are allowed by our framework. This might be relevant when using sliding mode controllers or similar discontinuous approaches providing finite-time convergence. The rationale behind (12)-(13) is that the velocity error dynamics in the coordinates $(\omega_e, \tilde{x}_c)$ is independent of w and τ_e. We formalize this requirement with the following Property.

Property 1 *(Internal model property). Given exosystem* (3)*, there exists a continuously differentiable function* ψ *and two outer semicontinuous* [1] *and locally bounded set-valued maps* Γ_c *and* Γ_ω *such that the stabilizers* γ_c, γ_ω *satisfies* (12) *and* (13)*, respectively.*

Based on Property 1, we may remove the dependence on τ_e of (11a) by using the shifted velocity coordinates $(\omega_e, \tilde{x}_c)$. However, to have a fully autonomous error system representation, we need also to remove the "external" input ω_v from (11a). To this end, as noted in [8], a possible strategy is to resort to the boundedness of $hK_R\varepsilon_e$ and the uniform boundedness of ω_d in Assumption 1. In particular, these properties imply that there exists a uniform bound $\omega_M > 0$ on $\omega_v(t)$, namely that the following quantity is finite:

$$\omega_M := \sup_{\substack{t \geq 0, q_e \in \mathbb{S}^3 \\ h \in \{-1,1\}}} \| -hK_R\varepsilon_e + \mathcal{R}(q_e)^\top \omega_d(t)\|. \tag{14}$$

Exploiting this bound, all solutions to (11) can be embedded in the larger funnel of solutions of the following hybrid inclusion:

$$\left.\begin{aligned} \dot{h} &= 0 \\ \dot{q}_e &= -W(q_e)(hK_R\varepsilon_e + \omega_e) \\ \begin{bmatrix} \dot{\omega}_e \\ \dot{\tilde{x}}_c \end{bmatrix} &\in F_\omega(\omega_e, \tilde{x}_c) \end{aligned}\right\} \quad (h, q_e, \omega_e) \in C \tag{15a}$$

$$\left.\begin{aligned} h^+ &= -h \\ q_e^+ &= q_e \\ \omega_e^+ &= \omega_e + 2hK_R\varepsilon_e \\ \tilde{x}_c^+ &= \tilde{x}_c \end{aligned}\right\} \quad (h, q_e, \omega_e) \in D. \tag{15b}$$

where

$$F_\omega(\omega_e, \tilde{x}_c) := \mathrm{co} \bigcup_{\|\omega_v\| \leq \omega_M} \begin{bmatrix} -J^{-1}\Gamma_\omega(\tilde{x}_c, \omega_e, \omega_v) \\ \Gamma_c(\tilde{x}_c, \omega_e, \omega_v) \end{bmatrix}, \tag{16}$$

with $\mathrm{co}(\cdot)$ denoting the convex hull. Also note that C and D in (7) and (11) being independent of x_c ensures that they remain unchanged in the error system (15).

Remark 2 *The structure of hybrid system* (15) *does not depend on the chosen coordinates to represent the attitude*

[1] Outer semicontinuity corresponds to the map having a closed graph [7, Lemma 5.10].

but only on the given (hierarchical) control architecture. While we use unit quaternions for the reasons mentioned in the Introduction, the closed-loop stability analysis proposed in the next section would follow the same ideas also for other representations possibly avoiding issues related to double-covering.

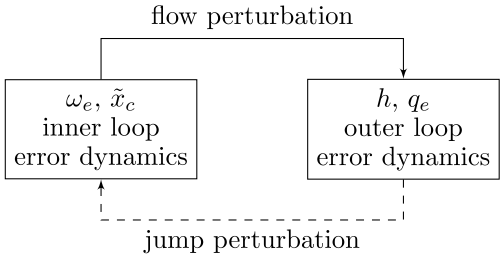

Fig. 2. Closed-loop error dynamics.

3.3 Selection of C, D and main stability theorem

In view of the double covering of SO(3) by $\mathbb{S}^3$, since both q_I and $-q_I$ correspond to the identity rotation matrix, following [13], the tracking objective in Problem 1 can be cast as the (robust) global asymptotic stabilization of the compact set

$$\mathcal{A} := \mathcal{A}_q \times \mathcal{A}_\omega, \tag{17}$$

for the closed loop (15), where $\mathcal{A}_q := \{(h, q_e) \in \{-1, 1\} \times \mathbb{S}^3 : q_e = hq_I\}$, $\mathcal{A}_\omega := \{(\omega_e, \tilde{x}_c) \in \mathbb{R}^3 \times \mathbb{R}^{n_c} : \omega_e = 0,\ \tilde{x}_c = 0\}$. In particular, the following statement is a straightforward consequence of the derivations of the previous sections.

Lemma 2 *If the set $\mathcal{A}$ is globally asymptotically stable for* (15)*, then controller* (7) *solves Problem 1 for the class of disturbances described by the exosystem* (3)*.*

Rather than providing a single solution to Problem 1, we parametrize here a set of possible solution approaches, requiring the following stabilization property from the controller dynamics γ_c and γ_ω. Two relevant selections satisfying the next property are illustrated in Section 4.

Property 2 *(Stabilization Property). The inner loop stabilizers γ_ω, γ_c satisfy Property 1 for some suitable selections of Γ_c and Γ_ω. Moreover, there exist a continuously differentiable positive definite and radially unbounded function $(\omega_e, \tilde{x}_c) \mapsto V_\omega(\omega_e, \tilde{x}_c)$, a diagonal matrix $K_\omega = diag(k_{\omega_1}, k_{\omega_2}, k_{\omega_3}) > 0$, and a continuous function $(\omega_1, \omega_2) \mapsto \delta_\omega(\omega_1, \omega_2)$ satisfying $\delta_\omega(0, 0) = 0$, such that*

$$V_\omega(\omega_1 + \omega_2, \tilde{x}_c) - V_\omega(\omega_1, \tilde{x}_c) \leq \delta_\omega(\omega_1, \omega_2), \quad \forall \omega_1, \omega_2, \tilde{x}_c, \tag{18}$$

$$\max_{f \in F_\omega(\omega_e, x_c)} \langle \nabla V_\omega(\omega_e, x_c), f \rangle \leq -\omega_e^\top K_\omega \omega_e, \quad \forall \omega_e, \tilde{x}_c. \tag{19}$$

Furthermore, no complete solution to $(\dot{\omega}_e, \dot{\tilde{x}}_c) \in F_\omega(\omega_e, \tilde{x}_c)$ can evolve forever in the set $\{(\omega_e, \tilde{x}_c) \in \mathbb{R}^3 \times \mathbb{R}^{n_c} : \omega_e = 0\}$, unless it is identically zero.

With Property 2 we establish bounds on the variation of V_ω along flowing and jumping solutions of the inner loop component of the error dynamics (15). Using these bounds we are ready to define the jump and flow sets C and D appearing in (7) and (15), thereby completing the construction of our hybrid controller. Let us first introduce the positive scalars:

$$k_V > \max_{i=1,2,3} (4 k_{\omega_i} k_{R_i})^{-1}, \quad \delta \in (0, 1), \tag{20}$$

and select C and D as the following closed sets:

$$\begin{aligned} C &:= \{(h, q_e, \omega_e) : 4(h\eta_e + \delta) + k_V \delta_\omega(\omega_e, 2hK_R\varepsilon_e) \geq 0\} \\ D &:= \{(h, q_e, \omega_e) : 4(h\eta_e + \delta) + k_V \delta_\omega(\omega_e, 2hK_R\varepsilon_e) \leq 0\}\,. \end{aligned} \tag{21}$$

Based on the construction completed above, we are now ready to state the main stability result of this paper.

Theorem 3 *For any γ_ω and γ_c satisfying Property 1 and Property 2 and any k_V and δ satisfying* (20)*, the attractor $\mathcal{A}$ in* (17) *is uniformly globally asymptotically stable for the error dynamics* (15)*,* (21)*.*

Due to Lemma 2, the global asymptotic stability result established in Theorem 3 implies that the proposed controller (7) with jump/flow sets as in (21), solves Problem 1 in the sense that with this controller, for any disturbance torque τ_e generated by exosystem (3), and for any desired trajectory $t \mapsto (R_d(t), \omega_d(t)) \in \text{SO}(3) \times \mathbb{R}^3$ satisfying Assumption 1, the corresponding attitude is uniformly asymptotically tracked from any initial condition. This fact is stated in the next corollary.

Corollary 4 *For any γ_ω and γ_c satisfying Property 2 and any k_V and δ satisfying* (20)*, controller* (7)*,* (21) *solves the robust attitude tracking Problem 1.*

A relevant structural property enjoyed by our solution is that it satisfies the hybrid basic conditions of [7, As. 6.5], which in turn imply the well-posedness property studied in [7, Ch. 6,7]. This fact is stated next and is a necessary step towards proving Theorem 3.

Lemma 5 *For any γ_ω and γ_c satisfying Property 2, the error dynamics* (15)*,* (21) *satisfies the hybrid basic conditions of [7, As. 6.5].*

Remark 3 *According to Theorem 3, the proposed design guarantees UGAS of the equilibrium set* (17) *for any choice of the parameters δ and k_V as in* (20)*. Therefore,* *the control law avoids the unwinding problem*[2] *by design. More specifically, the uniform convergence ensured by UGAS avoids arbitrary long transients emphasized.*

Remark 4 *Tuning of δ and k_V helps assigning a desirable transient when starting "far" from the equilibrium set $\mathcal{A}$: the switching mechanism ruled by δ and k_V essentially selects what quaternion point the solution should approach. As noted in [13], values of δ too close to the upper limit $\delta = 1$ may induce long transient, but values of δ too close to the lower limit $\delta = 0$ may lead to undesired chattering-like jumps with noisy measurements. As a consequence, δ should be selected as a suitable trade-off, depending on the measurement noise level. In practice, a value of $\delta = 0.5$ typically works well. The role of k_V is to also take into account the kinetic effects captured by V_ω, so that switches are partly inhibited if the velocity points the correct direction. In practice, it is reasonable to choose k_V close to the lower bounds in* (20)*, so that this inhibition is not too pronounced, thereby avoiding undesirable long transients.*

3.4 Proof of Theorem 3

The proof of Theorem 3 is based on the following corollary of [18, Thm 1], which we state here without proof.

Proposition 6 *Consider a compact set $\mathcal{A}$ and hybrid system* (15)*, satisfying the hybrid basic conditions of [7, As. 6.5]. Assume that there exists a continuously differentiable function V, positive definite with respect to $\mathcal{A}$ and radially unbounded, such that*

$$\dot V(x) := \langle \nabla V(x), \dot x\rangle \le 0, \qquad \forall x \in C \times \mathbb{R}^{n_c}, \quad \text{(22a)}$$
$$\Delta V(x) := V(x^+) - V(x) \le 0, \quad \forall x \in D \times \mathbb{R}^{n_c}. \quad \text{(22b)}$$

Assume also that no complete solution of (15) *keeps V constant and nonzero, namely no complete solution ϕ_{bad} exists satisfying $V(\phi_{bad}(t,j)) = V(\phi_{bad}(0,0)) \neq 0$ $\forall (t,j) \in dom(\phi_{bad})$. Then $\mathcal{A}$ is robustly uniformly globally asymptotically stable.*

We are now ready to prove Theorem 3, by exploiting Proposition 6 with the Lyapunov function candidate

$$V(x) := 2(1 - h\eta_e) + k_V V_\omega(\omega_e, \tilde x_c), \qquad (23)$$

in which the first (kinematic) component is inspired by [13]. Due to the properties of V_ω in Property 2, function V in (23) is positive definite with respect to $\mathcal{A}$ and radially unbounded. Let us now characterize the time derivative of V along flowing solutions to (15). We have

$$\dot V(x) = -2h\dot\eta_e + k_V \dot V_\omega = -2h\dot\eta_e + k_V\langle \nabla V_\omega(\omega_e, \tilde x_c), f\rangle \qquad (24)$$

where $f \in F_\omega(\omega_e, \tilde x_c)$. Hence, we can derive the following chain of inequalities based on (19),

$$\begin{aligned}\dot V(x) &\le -2he_1^\top W(q_e)(-hK_R\varepsilon_e - \omega_e) - k_V\omega_e^\top K_\omega \omega_e \\ &= h\varepsilon_e^\top(-hK_R\varepsilon_e - \omega_e) - k_V\omega_e^\top K_\omega\omega_e \\ &\le -\sum_{i=1}^{3} \begin{bmatrix} |\varepsilon_{e_i}| \\ |\omega_{e_i}| \end{bmatrix}^\top \begin{bmatrix} k_{R_i} & -\frac{1}{2} \\ -\frac{1}{2} & k_V k_{\omega_i} \end{bmatrix} \begin{bmatrix} |\varepsilon_{e_i}| \\ |\omega_{e_i}| \end{bmatrix} \le -\alpha_V \| \left[\begin{smallmatrix} \varepsilon_e \\ \omega_e \end{smallmatrix}\right] \|^2,\end{aligned} \qquad (25)$$

where $\alpha_V > 0$ is a small enough scalar constant, whose existence is guaranteed by the fact that, by design of k_V in (20), we have $4k_V k_{\omega_i} k_{R_i} > 1$ for all $i = 1, 2, 3$. Consider now the variation of V across jumps and let us use (21) and (18) to obtain, for all $x \in D$,

$$\begin{aligned}\Delta V(x) := V(x^+) - V(x) &= 2(1 - h^+\eta_e) + k_V V_\omega(\omega_e^+, \tilde x_c) \\ &\quad - 2(1 - h\eta_e) - k_V V_\omega(\omega_e, \tilde x_c) \\ &\le 4h\eta_e + k_V(V_\omega(\omega_e + 2hK_R\varepsilon_e, \tilde x_c) - V_\omega(\omega_e, \tilde x_c)) \\ &\le 4h\eta_e + k_V\delta_\omega(\omega_e, 2hK_R\varepsilon_e) \le -4\delta. \end{aligned} \qquad (26)$$

Based on (25) and (26), we can now apply Proposition 6 to complete the proof using function V in (23), which is continuously differentiable, positive definite with respect to $\mathcal{A}$ and radially unbounded, due to Property 2. The flow and jump inequalities in (22) follow directly from (25) and (26), therefore it remains to show that no solution ϕ_{bad} exists keeping V constant and nonzero. To this end, first note that (26) with its strict decrease, implies that such a solution, if it exists, can never jump and must be continuous. From (25), ϕ_{bad} must evolve forever in the set where both ε_e and ω_e are zero (in this set we have $\dot V(x) = 0$), however from the last statement in Property 2 and the cascade structure of the flow dynamics, ϕ_{bad} must necessarily evolve in the set where ε_e, ω_e and $\tilde x_c$ are all zero. This implies that $(\omega_e, \tilde x_c) \in \mathcal{A}_\omega$ and that $q_e = \left[\begin{smallmatrix} \eta_e \\ \varepsilon_e \end{smallmatrix}\right] \equiv \left[\begin{smallmatrix} -h \\ 0 \end{smallmatrix}\right]$ for some $h \in \{-1, 1\}$ (as a matter of fact, these are the only two points in $\{-1,1\} \times \mathbb{S}^3$ outside $\mathcal{A}_q$ and where $\varepsilon_e = 0$). Replacing these constraints in the definition of the flow/jump condition in (21), one obtains $4(h\eta_e + \delta) + k_V\delta_\omega(\omega_e, 2hK_R\varepsilon_e) = 4(\delta - 1) < 0$, where we exploited $h^2 = 1$, the identity $\delta_\omega(0,0) = 0$ from Property 2, and the fact that $\delta < 1$. The above inequality implies that neither of those two points are in the flow set, where continuous evolution is allowed, thereby proving that the solution ϕ_{bad} does not exist and completing the proof.

4 Sample stabilizers design

To illustrate the generality of our control scheme we list here two possible selections of the controller function

[2] Unwinding is the problem for which solutions starting close to one of the two points in $\mathcal{A}$ experience a large overshoot because they are (unreasonably) forced to approach the other point (due to the double coverage of quaternions, these two points represent the same physical attitude, see, *e.g.*, [13]).

γ_ω and γ_c satisfying Property 1 and 2, thereby guaranteeing the applicability of Theorem 3. In particular, we consider: A) a stabilizer robust to harmonic disturbances, B) a conditional integrator, which is a dynamic controller embedding a proportional-integral action with anti-windup to reject constant disturbances.

4.1 Harmonic disturbances compensator

Non-global (and non-uniform) attitude tracking with a disturbance torque τ_e comprising a linear combination of constant and harmonic signals with known frequencies but unknown amplitudes and phases has been addressed in [17], where a continuous control law induces almost global results. In this Section we show how the problem of harmonic disturbances can be solved globally (and uniformly) by our solution. Any such disturbance can be generated by the exosystem (3) with

$$s(w) = A_w w, \quad \tau(w) = C_w w, \tag{27}$$

where

$$A_w = \text{blkdiag}\left(0, \left[\begin{smallmatrix} 0 & -\Omega_1 \\ \Omega_1 & 0 \end{smallmatrix}\right], \cdots, \left[\begin{smallmatrix} 0 & -\Omega_{n_d} \\ \Omega_{n_d} & 0 \end{smallmatrix}\right]\right) \tag{28}$$

and $C_w \in \mathbb{R}^{3\times 3+n_d}$ are assumed to be an observable pair and Ω_i, $i \in \{1, 2, \ldots, n_d\}$, are known frequencies. The ensuing dynamics is marginally stable in the sense that it generates a homogeneous family of closed bounded orbits and we can select $\mathcal{W}$ as the union of all the possible orbits generated by bounded initial conditions $|w(0)| \leq w_M$, where w_M is not required for the control design. Assuming the initial condition $w(0)$ be unknown is equivalent to assuming the amplitudes and phases of the harmonic components be unknown. We propose the internal model-based controller selection:

$$\begin{aligned} \gamma_c(x_c, \omega_e, \omega_v) &:= A_w x_c + K_c C_w^\top \omega_e \\ \gamma_\omega(x_c, \omega_e, \omega_v) &:= C_w x_c + K_\omega \omega_e + S(\omega_e) J(\omega_v - \omega_e) \\ \delta_\omega(\omega_1, \omega_2) &:= \tfrac{1}{2}\omega_2^\top J(\omega_2 + 2\omega_1) \end{aligned} \tag{29}$$

with the tunable matrix $K_c = \text{blkdiag}(K_I, k_{c_1} I_2, \ldots, k_{c_d} I_2) \in \mathbb{R}_{>0}^{3+n_d\times 3+n_d}$, $K_I = \text{diag}(k_{I_1}, k_{I_2}, k_{I_3}) \in \mathbb{R}_{>0}^{3\times 3}$, $k_{c_i} > 0$ $\forall i \in \{1, 2, \ldots, d\}$. For this special case, a simple single-valued selection of the set-valued maps

$$\begin{aligned} \Gamma_c(\tilde{x}_c, \omega_e, \omega_v) &:= \{\gamma_c(\tilde{x}_c, \omega_e, \omega_v)\},\ \forall \tilde{x}_c, \omega_e, \omega_v \\ \Gamma_\omega(\tilde{x}_c, \omega_e, \omega_v) &:= \{\gamma_\omega(\tilde{x}_c, \omega_e, \omega_v)\},\ \forall \tilde{x}_c, \omega_e, \omega_v, \end{aligned} \tag{30}$$

is enough for proving that controller (29) satisfies Property 1 and Property 2, as established next.

Proposition 7 *Given the exosystem* (27)-(28)*, selections* (29) *satisfy Property 1 and Property 2 with* $\psi(w) := -w$ *and* Γ_c, Γ_ω *in* (30)*. Then, from Corollary 4, controller* (7)*,* (21) *with* (29) *solves Problem 1 for any disturbance torque* τ_e *generated by* (3) *with* (27)*.*

Sketch of the proof. Using the error coordinate $\tilde{x}_c := x_c - \psi(w)$, where $\psi(w) = -w$, the linearity of γ_c and γ_ω in (29) immediately proves (12) and (13) (thus, Property 1) with the trivial selection (30). For the the proof of Property 2, one can use the Lyapunov function $V_\omega(\omega_e, \tilde{x}_c) := \frac{1}{2}\left[\begin{smallmatrix} \omega_e \\ \tilde{x}_c \end{smallmatrix}\right]^\top \left[\begin{smallmatrix} J & 0 \\ 0 & K_c^{-1} \end{smallmatrix}\right] \left[\begin{smallmatrix} \omega_e \\ \tilde{x}_c \end{smallmatrix}\right]$ for which it holds that $\dot{V}_\omega(\omega_e, \tilde{x}_c) \leq -\omega_e^\top K_\omega \omega_e$, thereby proving (19). The use of an invariance argument similar to the one used in the proof of [8, Proposition 2] allows proving the last part of Property 2. □

Remark 5 *By virtue of the modular architecture of our control law it is possible to extend our scheme to the case of three independent harmonic disturbances with unknown frequencies (in addition to unknown amplitudes and phases), which can be generated by the exosystem in* (27) *with* $C_w = \mathit{blkdiag}(c_{w_1}^\top, c_{w_2}^\top, c_{w_3}^\top)$ *and* $A_w = \mathit{blkdiag}(A_{w_1}, A_{w_2}, A_{w_3})$*,* $A_{w_i} := \left[\begin{smallmatrix} 0 & -\Omega_i \\ \Omega_i & 0 \end{smallmatrix}\right]$*, where* $c_{w_i} \in \mathbb{R}^2$ *and* Ω_i*,* $i \in \{1, 2, 3\}$*, are unknown constant terms. For this case, based on the adaptive observer construction of [16], we can consider the selection:*

$$\begin{aligned} \gamma_{c_i}(x_c, \omega_e, \omega_v) &:= \begin{bmatrix} A_{o_i}\hat{\zeta}_i - b_{o_i}\left(k_{\omega_i}\omega_{e_i} - \hat{\theta}_i^\top \hat{\zeta}_i + \omega_{e_i}\right) \\ -k_{c_i}\hat{\zeta}_i \omega_{e_i} \end{bmatrix} \\ \gamma_{\omega_i}(x_c, \omega_e, \omega_v) &:= k_{\omega_i}\omega_{e_i} - \hat{\theta}_i^\top \hat{\zeta}_i + \omega_{e_i} \\ \delta_\omega(\omega_1, \omega_2) &:= \tfrac{1}{2}\omega_2^\top J(\omega_2 + 2\omega_1), \end{aligned} \tag{31}$$

$\forall i \in \{1, 2, 3\}$*, where* $x_{c_i} = \left[\begin{smallmatrix} \eta_i^\top & \hat{\theta}_i^\top \end{smallmatrix}\right]^\top \in \mathbb{R}^{2+2}$ *,* $\hat{\zeta}_i := \eta_i - b_{o_i} J_i \omega_{e_i}$*, the pair* $(A_{o_i}, b_{o_i}) \in \mathbb{R}_{<0}^{2\times 2} \times \mathbb{R}^2$ *satisfies* $M_i A_{w_i} - A_{o_i} M_i = b_{o_i} c_{w_i}^\top$ *for some non-singular matrix* $M_i \in \mathbb{R}^{2\times 2}$*,* $k_{c_i} > 0$ *is the adaptation gain and* $J = \text{diag}(J_1, J_2, J_3)$ *(principal axes body frame). A generalized version of Proposition 7 can be proven also for this uncertain case but is not reported here due to length restrictions (see the [9] for a detailed derivation). Simulation results showing the benefit of this solution over the standard design in* (29)*, when the disturbance frequencies are uncertain, are reported in Section 5.*

4.2 Conditional integrators for constant disturbances

We address here a nonlinear construction with the disturbance torque τ_e in (2) being constant and unknown. The corresponding parameters of the exosystem (3) are

$$s(w) = 0, \quad \tau(w) = w, \tag{32}$$

with $w \in \mathbb{R}^3$. For this special case, we designed in our preliminary work [8] a PI-type controller. Here we enhance that design by embedding in it a structural anti-windup action, stemming from the so-called conditional integrator paradigm (see, *e.g.*, [4]), which effectively removes the integral windup issues, as illustrated in Section 5. Inspired by [4], we select the controller

$$
\begin{aligned}
\gamma_c(x_c,\omega_e,\omega_v) &:= -Gx_c + H\sigma \\
\gamma_\omega(x_c,\omega_e,\omega_v) &:= K_\omega\omega_e + F\sigma + S(\omega_e)J(\omega_v-\omega_e) \\
\sigma &= \mathrm{sat}(H^{-1}(Gx_c+\omega_e)) \\
\delta_\omega(\omega_1,\omega_2) &:= \tfrac{1}{2}\omega_2^\top J(\omega_2+2\omega_1),
\end{aligned} \tag{33}
$$

where $G = \mathrm{diag}(g_1,g_2,g_3) \in \mathbb{R}^{3\times3}_{>0}$, $H = \mathrm{diag}(h_1,h_2,h_3) \in \mathbb{R}^{3\times3}$, $F = \mathrm{diag}(f_1,f_2,f_3) \in \mathbb{R}^{3\times3}_{>0}$, $K_\omega \in \mathbb{R}^{3\times3}$ and $\mathrm{sat}(\cdot)$ denotes the decentralized unit saturation function (defined in the notation section). Due to the presence of saturation in γ_ω in (33), the components of the disturbance torque which can be compensated by the controller cannot be larger than the diagonal elements of $F > 0$. Therefore, we define the compact set characterizing the exosystem (3), (32) as

$$
\mathcal{W} := \{w \in \mathbb{R}^3 : |w_i| \le (1-\epsilon)f_i,\ i=1,2,3\}, \tag{34}
$$

where $0<\epsilon<1$ is a scalar providing some margin to the stabilizer. Notice that this scalar is associated with the robustness/performance trade-off because, for a given selection of F, it sets the maximum size of the allowable disturbance (the robustness side), versus the input margin available for stabilization (the performance side). The effectiveness of the controller selection (33) can be proven by more sophisticated choices of set-valued maps Γ_c and Γ_ω in (12) and (13). In particular, we propose to use, for each x_c,ω_e,ω_v,

$$
\begin{aligned}
\Gamma_c(\tilde{x}_c,\omega_e,\omega_v) &:= -G\tilde{x}_c + H\Sigma(\tilde{x}_c,\omega_e), \\
\Gamma_\omega(\tilde{x}_c,\omega_e,\omega_v) &:= K_\omega\omega_e + F\Sigma(\tilde{x}_c,\omega_e) + S(\omega_e)J(\omega_v-\omega_e), \\
\Sigma(\tilde{x}_c,\omega_e) &:= \bigcup_{M\ge\varepsilon} \mathrm{sat}_M(H^{-1}(G\tilde{x}_c+\omega_e)),
\end{aligned} \tag{35}
$$

which is outer semicontinuous because its graph is a union of closed graphs (continuous functions) and locally bounded because of local boundedness of the argument of the saturation. With this selection, we prove below that controller (33) satisfies Properties 1 and 2, thereby solving Problem 1, thanks to Corollary 4.

Proposition 8 *Given the exosystem* (32),(34)*, selections* (33)*, satisfy Property 1 and Property 2 with* $\psi(w) = -G^{-1}HF^{-1}w$ *and* Γ_c,Γ_ω *in* (35)*. Then, from Corollary 4, controller* (7),(21) *with* (33) *solves Problem 1 for any disturbance torque* τ_e *generated by* (3) *with* (32),(34)*.*

Proof. Using the error coordinates $\tilde{x}_c := x_c - \psi(w)$, where $\psi(w) = -G^{-1}HF^{-1}w$, we obtain the following expression for the functions at the left-hand side of (12) and (13):

$$
\begin{aligned}
\gamma_c(\tilde{x}_c+\psi(w),\omega_e,\omega_v) - \mathrm{D}\psi s(w) &= -G\tilde{x}_c + H\widetilde{\sigma} \\
\gamma_\omega(\tilde{x}_c+\psi(w),\omega_e,\omega_v) + \tau(w) &= K_\omega\omega_e + F\widetilde{\sigma} \\
&\quad + S(\omega_e)J(\omega_v-\omega_e)
\end{aligned} \tag{36}
$$

$$
\widetilde{\sigma} := \mathrm{sat}(H^{-1}(G\tilde{x}_c+\omega_e) - F^{-1}w) + F^{-1}w, \tag{37}
$$

and due to the property of w in (34), we have that $\widetilde{\sigma} \in \Sigma(\tilde{x}_c,\omega_e)$ in (35), because the term $F^{-1}w$, which satisfies $|F^{-1}w| \le 1-\varepsilon$, leaves enough margin for the saturation function $\mathrm{sat}(\cdot)$. This proves (12) and (13) with selections (35) and thus Property 1. Let us now focus on Property 2. Using (35), we study the following differential inclusion, issued from (16),

$$
\begin{bmatrix}\dot{\omega}_e \\ \dot{\tilde{x}}_c\end{bmatrix} \in \bigcup_{\substack{\|\omega_v\|\le\omega_M \\ \widetilde{\sigma}\in\Sigma(\omega_e,\tilde{x}_c)}} \begin{bmatrix} J^{-1}(S(\omega_e)J(\omega_e-\omega_v) - K_\omega\omega_e - F\widetilde{\sigma} \\ -G\tilde{x}_c + H\widetilde{\sigma}\end{bmatrix}, \tag{38}
$$

where the right-hand side is already convex, due to the convexity of Σ and because ω_v enters linearly the dynamics. To verify (18)-(19), we use the quadratic function

$$
V_\omega(\omega_e,\tilde{x}_c) := \frac{1}{2}\begin{bmatrix}\omega_e \\ \tilde{x}_c\end{bmatrix}^\top \begin{bmatrix} J & 0 \\ 0 & P_c\end{bmatrix}\begin{bmatrix}\omega_e \\ \tilde{x}_c\end{bmatrix}, \tag{39}
$$

where $P_c \in \mathbb{R}^{n_c\times n_c}_{>0}$ is selected below. First note that (18) holds straightforwardly, with an equality sign, when using δ_ω in (33). Let us now prove (19) by computing $\dot{V}_\omega(\omega_e,\tilde{x}_c) = \langle\nabla V_\omega(\omega_e,x_c), f\rangle$ for any $f \in F_\omega(\omega_e,x_c)$. Using (38), we obtain:

$$
\begin{aligned}
&\dot{V}_\omega(\omega_e,\tilde{x}_c) = -\omega_e^\top K_\omega\omega_e - \omega_e^\top F\widetilde{\sigma} \\
&- \frac{1}{2}\tilde{x}_c^\top\left(P_cG + G^\top P_c\right)\tilde{x}_c + \tilde{x}_c^\top P_cH\widetilde{\sigma},\ \ \widetilde{\sigma}\in\Sigma(\tilde{x}_c,\omega_e),
\end{aligned} \tag{40}
$$

where we exploited the property $\omega_e^\top S(\omega_e)^\top J(\omega_v-\omega_e) = (J(\omega_v-\omega_e))^\top S(\omega_e)\omega_e = 0$ (because $S(\omega_e)\omega_e = 0$). To manipulate (40), recalling that $\widetilde{\sigma}\in\Sigma(\tilde{x}_c,\omega_e)$, from the expression of $\Sigma(\tilde{x}_c,\omega_e)$ in (35) and the sector properties of the saturation, it holds that, for any $W>0$ diagonal,

$$
\widetilde{\sigma}^\top W(H^{-1}(G\tilde{x}_c+\omega_e) - \widetilde{\sigma}) \ge 0. \tag{41}
$$

With the goal in mind of canceling out the last term in the first row of (40), select $W = FH$ in (41) to obtain

$$
\begin{aligned}
\dot{V}_\omega(\omega_e,\tilde{x}_c) &\le \dot{V}_\omega(\omega_e,\tilde{x}_c) + \widetilde{\sigma}^\top W(H^{-1}(G\tilde{x}_c+\omega_e) - \widetilde{\sigma}) \\
&= -\omega_e^\top K_\omega\omega_e + \Psi(\tilde{x}_c,\widetilde{\sigma}).
\end{aligned} \tag{42}
$$

Since F, G and H are diagonal and positive definite, by selecting $P_c = GH^{-1}F$, it can be shown that function Ψ satisfies:

$$
\begin{aligned}
\Psi(\tilde{x}_c,\widetilde{\sigma}) &= -\tilde{x}_c^\top P_cG\tilde{x}_c + \tilde{x}_c^\top P_cH\widetilde{\sigma} + \widetilde{\sigma}^\top FG\tilde{x}_c - \widetilde{\sigma}^\top FH\widetilde{\sigma} \\
&= -\begin{bmatrix}\tilde{x}_c \\ \widetilde{\sigma}\end{bmatrix}^\top \begin{bmatrix} G \\ -H\end{bmatrix} H^{-1}F\begin{bmatrix} G & -H\end{bmatrix}\begin{bmatrix}\tilde{x}_c \\ \widetilde{\sigma}\end{bmatrix} \le 0.
\end{aligned}
$$

Combining this last inequality with (42), we obtain (19). To prove the last part of Property 2, we proceed in a similar way to the end of the proof of Proposition 7. Consider any solution $t \mapsto x_\omega(t) := (\omega_e(t), \tilde{x}_c(t))$ to (38) and assume, by contradiction, that it starts and only evolves in the set $\mathcal{G} := \{(\omega_e, \tilde{x}_c) \in \mathbb{R}^3 \times \mathbb{R}^{n_c} : \ \omega_e = 0\} \setminus \{(0,0)\}$. Then, the expression of dynamics (38) restricted to $\mathcal{G}$, corresponds to

$$\begin{bmatrix} \dot{\omega}_e \\ \dot{\tilde{x}}_c \end{bmatrix} \in F_\omega(\mathcal{G}) = \bigcup_{\widetilde{\sigma} \in \Sigma(\tilde{x}_c, 0)} \begin{bmatrix} -J^{-1}F\widetilde{\sigma} \\ -G\tilde{x}_c + H\widetilde{\sigma} \end{bmatrix}, \qquad (43)$$

where $\widetilde{\sigma}$ can never be zero because the set-valued map $\Sigma(\tilde{x}_c, 0) = \bigcup_{M \geq \varepsilon} \mathrm{sat}_M(H^{-1}G\tilde{x}_c)$ does not contain the zero element, due to the fact that $\tilde{x}_c \neq 0$ and $H^{-1}G$ is diagonal positive definite. Finally, since $J^{-1}F$ is nonsingular, we have $\dot{\omega}_e \neq 0$ and ω_e cannot remain identically zero, completing the proof of Property 2 and the proof of the lemma. □

5 Numerical results

In this section a simulation example is presented to show that the control law (7) with the selections proposed in Section 4 solves the robust tracking problem in the presence of constant and harmonic disturbances τ_e in (2). The desired attitude trajectory is characterized by a periodic motion described, in terms of Euler angles, by $(\phi_d(t), \theta_d(t), \psi_d(t)) = (\sin(\omega_{d_1}t), \sin(\omega_{d_2}t), \sin(\omega_{d_3}t))$, where $\omega_d = \left[\begin{smallmatrix} 0 & 1 & 0.5 \end{smallmatrix}\right]^\top$ rad/s . The inertia matrix of the rigid body is $J = \mathrm{diag}(1,2,3)\,\mathrm{kgm}^2$ and we assume a piece-wise smooth disturbance torque τ_e defined as $\tau_e(t) = \left[\begin{smallmatrix} 1 & 1 & 1 \end{smallmatrix}\right]^\top$ Nm if $t \leq 15$s, $\tau_e(t) = -\left[\begin{smallmatrix} 2 & 2 & 2 \end{smallmatrix}\right]^\top$ Nm if $15 < t \leq 25$s and $\tau_e(t) = -\left[\begin{smallmatrix} 2\cos(t-25) & 2 & 2 \end{smallmatrix}\right]^\top$ Nm if $t \geq 25$s. The initial state that we consider corresponds to a 180deg rotation about the roll axis, namely, $R_e(0) = I_3 + \sin(\pi)S(e_1) + (1 - \cos(\pi))S(e_1)^2$, and to a significant angular velocity error $e_\omega(0) := \omega(0) - R_e^\top(0)\omega_d(0) = \left[\begin{smallmatrix} 3 & 3 & 0.5 \end{smallmatrix}\right]^\top$ rad/s with respect to the target velocity.

The gains of the conditional integrator-based controller (in short, CI) are tuned to have a predefined behavior of the closed-loop system in the proximity of the desired attitude motion. Specifically, the gains of the inner loop stabilizers are chosen such that the linearized inner loop error dynamics for $\omega_d = 0$, $J_i\dot{\omega}_{e_i} = \bar{k}_{\omega_i}\omega_{e_i} + k_{I_i}x_{c_i}$, $\dot{x}_{c_i} = \omega_{e_i}$, corresponds to a second order system with bandwidth 3rad/s and critical damping. To this end, we set $\bar{k}_{\omega_i} = 2 \cdot 3J_i$ and $k_{I_i} = 3^2J_i$, which are obtained by choosing $F = \mathrm{diag}(4,4,4)$, $G = \mathrm{diag}(10, 10/J_2, 10/J_3)$, $H = \mathrm{diag}(4,4,4)$ and $K_\omega = G - FH^{-1}$ in (33). Since $f_i = 4\ \forall i \in \{1,2,3\}$, from (34), the magnitude of the disturbance torque that can be rejected should be less than $4Nm$ along each axis. As for the harmonic compensator (in short, HC), we set the tunable matrices in (29) as $A_w = \mathrm{blkdiag}\left(\mathrm{diag}(0,0,0), \left[\begin{smallmatrix} 0 & -2 \\ 2 & 0 \end{smallmatrix}\right]\right)$, $C_w = \left[\begin{smallmatrix} 1 & 0 & 0 & 1 & 0 \\ 0 & 1 & 0 & 0 & 0 \\ 0 & 0 & 1 & 0 & 0 \end{smallmatrix}\right]$ and, in order to have the same behavior as the CI controller in unsaturated conditions (for constant disturbances), we set the gains as $k_{\omega_i} = 2 \cdot 3J_i$, $k_{I_i} = 3^2J_i\ \forall i \in \{1,2,3\}$, and $k_{c_4} = 9$. The gains of the outer loop controller are tuned to have a 0.5rad/s bandwidth for the linearized outer loop error, which is achieved by setting $K_R = I_3$ in (10). Finally, for the hybrid logic in (21), we select $\delta = 0.25$ and $k_V = 0.75 > \max_{i=1,2,3}(4k_{\omega i}k_{Ri})^{-1} = 2/3$. Assuming that the actuators can provide a maximum control torque of $M = 5Nm$, the control output τ_c is saturated as $\tau_c^{sat} = \mathrm{sat}_M(\tau_c)$, where function $\mathrm{sat}_M(\cdot)$ is defined in the notation section.

The attitude tracking performance of the proposed controllers is illustrated in Figure 3 in terms of the normalized Euclidean distance in SO(3), *i.e.*, $\|R_e\|_{\mathrm{SO}(3)} = \sqrt{\frac{1}{4}(I_3 - R_e)}$. It is worth mentioning that for both controllers the logic variable h jumps at $t = 0$ since the initial conditions are both in the jump set. Due to the large initial error, the controllers require a large torque in the initial transient phase and both reach saturation. During the first transient, windup effects are clearly visible in the response of the HC controller while the CI controller achieves a faster transient without overshoot (Figure 3). Figure 4 shows that in the initial seconds of the simulation the control torque is kept in saturated conditions for a longer time when using the HC controller (just the third component is shown for space reasons). When the disturbance torque changes at $t = 15s$, the controllers respond similarly along the pitch and yaw axes, since they both operate in unsaturated conditions and their behavior is expected to be the same by design. A different response is observed as far as the roll axis is concerned, since the HC controller includes additional dynamics to reject harmonic disturbances acting along this axis. This point is clearly shown in the last part of the simulation ($t \geq 25s$), when the rigid body is affected by the harmonic component of τ_e: the HC controller achieves asymptotic rejection while the CI controller cannot reject the disturbance and bounded oscillations are present along all the axes due to the couplings.

Finally, Figure 5 shows the improvement, in terms of tracking performance, achieved by implementing the Adaptive Observer (AO) design given in (31) over the standard HC given in (29) when considering an imperfect knowledge of the disturbance frequencies. Specifically, we consider $\tau_e = \left[\begin{smallmatrix} \cos(2t) & 2\cos(3t) & 3\cos(t) \end{smallmatrix}\right]^\top$ Nm but assume $\Omega_i = 2$rad/s, $i \in \{1,2,3\}$, in A_w for (29). The parameters of the AO controller are chosen as $\Gamma_i = 10$, $A_{o_i} = \left[\begin{smallmatrix} 0 & 1 \\ -6 & -1 \end{smallmatrix}\right]$, $b_{o_i} = \left[\begin{smallmatrix} 0 & 1 \end{smallmatrix}\right]^\top$, $i \in \{1,2,3\}$. The other parameters are the same as the previous simulation.

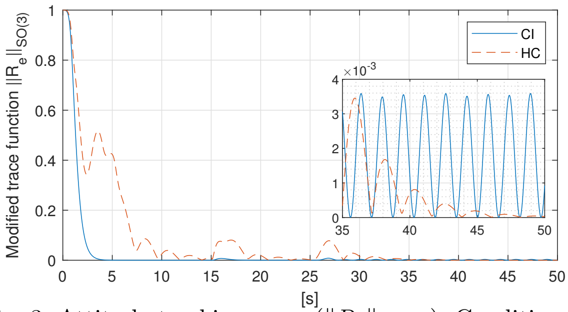

Fig. 3. Attitude tracking error ($\|R_e\|_{SO(3)}$). Conditional integrator (CI) *vs* Harmonic Controller (HC).

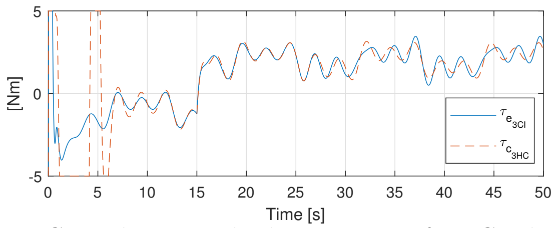

Fig. 4. Control torque: third component of τ_c. Conditional integrator (CI) *vs* Harmonic Controller (HC).

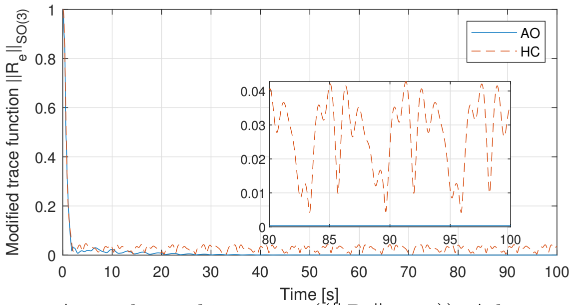

Fig. 5. Attitude tracking error (($\|R_e\|_{SO(3)}$)). Adaptive Observer (AO) *vs* standard Harmonic Controller (HC).

6 Conclusions

In this paper we considered the attitude tracking problem and proposed a control design with disturbance rejection capabilities. Our solution, based on an inner-outer loop paradigm, guarantees global tracking results which are achieved by including a hybrid logic to overcome the well-known topological issues of SO(3). Relying on an internal model description of the disturbances, we show that the proposed approach can be used to reject certain classes of torque disturbances of engineering interest. Leveraging the proposed approach, one can exploit dynamic controllers for the inner loop, such as PID loops, conditional integrators or harmonic compensators, to achieve desirable performance and disturbance rejection capabilities.

References

[1] S. Berkane, A. Abdessameud, and A. Tayebi. Hybrid attitude and gyro-bias observer design on SO(3). *IEEE Transactions on Automatic Control*, 62(11):6044–6050, November 2017.

[2] S. Berkane, A. Abdessameud, and A. Tayebi. Hybrid global exponential stabilization on SO(3). *Automatica*, 81:279 – 285, 2017.

[3] S. Berkane and A. Tayebi. Construction of synergistic potential functions on SO(3) with application to velocity-free hybrid attitude stabilization. *IEEE Transactions on Automatic Control*, 62(1):495–501, January 2017.

[4] M. Burger. *Disturbance Rejection using Conditional Integrators: Applications to path manoeuvring under environmental disturbances for single vessels and vessel formations.* PhD thesis, NTNU, 2011.

[5] P. Casau, R. Cunha, R. G. Sanfelice, and C. Silvestre. Hybrid control for robust and global tracking on smooth manifolds. *IEEE Transactions on Automatic Control*, 65(5):1870–1885, 2020.

[6] P. Casau, C. G. Mayhew, R. G. Sanfelice, and C. Silvestre. Robust global exponential stabilization on the n-dimensional sphere with applications to trajectory tracking for quadrotors. *Automatica*, 110:108534, 2019.

[7] R. Goebel, R. G. Sanfelice, and A. R. Teel. *Hybrid Dynamical Systems.* University Press Group Ltd, 2012.

[8] D. Invernizzi, M. Lovera, and L. Zaccarian. Hierarchical dynamic control design for robust attitude tracking. In *21st IFAC World Congress, Berlin, Germany*, 2020.

[9] D. Invernizzi, M. Lovera, and L. Zaccarian. Global robust attitude tracking with torque disturbance rejection via dynamic hybrid feedback. Report hal-03582289, 2022.

[10] T. Lee. Robust adaptive attitude tracking on SO(3) with an application to a quadrotor UAV. *IEEE Transactions on Control Systems Technology*, 21(5):1924–1930, 2013.

[11] T. Lee. Global exponential attitude tracking controls on SO(3). *IEEE Transactions on Automatic Control*, 60(10):2837–2842, 2015.

[12] D. H. S. Maithripala and J. M. Berg. An intrinsic PID controller for mechanical systems on Lie groups. *Automatica*, 54(4):189–200, 2015.

[13] C. G. Mayhew, R. G. Sanfelice, and A. R. Teel. Quaternion-based hybrid control for robust global attitude tracking. *IEEE Transactions on Automatic Control*, 56(11):2555–2566, 2011.

[14] C. G. Mayhew, R. G. Sanfelice, and Andrew R. Teel. On path-lifting mechanisms and unwinding in quaternion-based attitude control. *IEEE Transactions on Automatic Control*, 58:1179–1191, 2013.

[15] C. G. Mayhew and A. R. Teel. Synergistic hybrid feedback for global rigid-body attitude tracking on SO(3). *IEEE Transactions on Automatic Control*, 58:2730–2742, 2013.

[16] V.O. Nikiforov. Adaptive non-linear tracking with complete compensation of unknown disturbances. *European Journal of Control*, 4(2):132–139, 1998.

[17] A. Sanyal, A. Fosbury, N. Chaturvedi, and D. S. Bernstein. Inertia-free spacecraft attitude tracking with disturbance rejection and almost global stabilization. *Journal of Guidance, Control, and Dynamics*, 32(4):1167–1178, 2009.

[18] A. Seuret, C. Prieur, S. Tarbouriech, A. R. Teel, and L. Zaccarian. A nonsmooth hybrid invariance principle applied to robust event-triggered design. *IEEE Transactions on Automatic Control*, 64(5):2061–2068, May 2019.

[19] J. Su and K-Y. Cai. Globally stabilizing proportional-integral-derivative control laws for rigid-body attitude tracking. *Journal of Guidance, Control, and Dynamics*, 34(4):1260–1264, 2011.